DESIGN CONSTRAINTS FOR POLYNOMIAL AND RATIONAL FILTERS

Sabine Kröner

Center for Computing Technology
University of Bremen
P.O. Box 330440, 28334 Bremen, Germany
e-mail: kroener@informatik.uni-bremen.de

Giovanni Ramponi

Image Processing Laboratory, DEEI
University of Trieste
via A. Valerio 10, 34127 Trieste, Italy
e-mail: ramponi@univ.trieste.it

ABSTRACT

Polynomial and rational filters for image enhancement, edge preserving noise smoothing, and interpolation of encoded images are usually designed as a weighted combination of nonlinear filters having lowpass or highpass behaviour. The choice of the filter components and of the coefficients is performed heuristically, though.

In this paper general design constraints for polynomial and rational filters are presented that are necessary to achieve isotropy, the preservation of the expectation value, and the detection of edges. For the application of edge preserving noise smoothing a method is derived to find an optimal polynomial or rational filter that meets these constraints.

1. INTRODUCTION

Polynomial and rational filters have shown to be a successful tool for applications in image enhancement, edge preserving noise smoothing, and interpolation of encoded images [1, 4, 6, 7, 8, 9]. Their design is usually based on a weighted combination of nonlinear filters having lowpass or highpass behaviour where the choice of the filter components and of the coefficients is performed heuristically. This leads to filters that yield convincing results in experiments but leak a mathematical foundation. Constraints that have already been derived like the one for the preservation of the expected output of a uniform luminance [5] are only valid for special filters.

Here we present some generally applicable design constraints that are necessary to achieve certain properties of polynomial and rational filters. For the derivation of the constraints instead of the usual design approach based on low- and highpass filters we start from a general mathematic description of a polynomial filter.

2. POLYNOMIAL FILTERS

A general two-dimensional polynomial filter can be defined as

$$\begin{aligned} y_{0,0} &= c + \sum_{i,j=-N}^{N} w_{i,j} x_{i,j} + \sum_{i,j,k,l=-N}^{N} w_{i,j,k,l} x_{i,j} x_{k,l} + \\ & \sum_{i,j,k,l,m,n=-N}^{N} w_{i,j,k,l,m,n} x_{i,j} x_{k,l} x_{m,n} + \dots \end{aligned} \quad (1)$$

with a constant term c and weighting factors $w_{i,j}$, $w_{i,j,k,l}$, etc. This description comprises all multiplicative combinations up to a certain order between the pixels $x_{i,j}$ of a filter mask of size $(2N+1) \times (2N+1)$. For a filter mask of size 3×3, i.e. $N = 1$, the numbering of the filter elements is as shown in Figure 1.

$x_{-1,1}$	$x_{0,1}$	$x_{1,1}$
$x_{-1,0}$	$x_{0,0}$	$x_{1,0}$
$x_{-1,-1}$	$x_{0,-1}$	$x_{1,-1}$

Figure 1: Numbering of the filter elements in a 3×3 filter mask

3. CONSTRAINTS

3.1. Isotropy

One important desired property of the filter is isotropy. It can be obtained by using the same coefficients for all products of filter elements in eq. (1), so called monomials, that are of the same type but have different orientations.

A monomial f_m has the form $f_m := x_{i_1,j_1}^{b_1} \cdot x_{i_2,j_2}^{b_2} \cdot \ldots \cdot x_{i_n,j_n}^{b_n}$ with $b_i \in I\!N$. An example of monomials of the same type in different orientations are the monomials $x_{0,1}^2 x_{1,0}$, $x_{1,0}^2 x_{0,-1}$, $x_{0,-1}^2 x_{-1,0}$, and $x_{-1,0}^2 x_{0,1}$. They can be combined additively to one value which is afterwards weighted with one coefficient:

$$\mathrm{I13} = x_{0,1}^2 x_{1,0} + x_{1,0}^2 x_{0,-1} + x_{0,-1}^2 x_{-1,0} + x_{-1,0}^2 x_{0,1} \; . \quad (2)$$

I13 can also be interpreted as a *monomial filter kernel* based on the sum of monomials of third order. Its graphical visualization is shown in Figure 2.

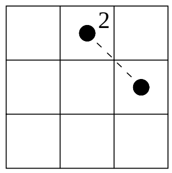

I13

Figure 2: Monomial filter kernel for I13

In the same way all other monomials derived from eq. (1) can be combined to monomial filter kernels. Table 1 shows as an example the 17 monomial filter kernels based on monomials of up to order three that are only composed of elements in vertical and horizontal direction with respect to $x_{0,0}$ in the 3×3 mask.

The isotropy constraint thus leads to a description of the filter as a linear combination of monomial filter kernels I_j of linear and higher order [2]. The output image $\boldsymbol{y}$ of a general polynomial filter applied on an image $\boldsymbol{x}$ can then be written as

$$\boldsymbol{y} = \boldsymbol{x} + \sum_{j=1}^{n} a_j \mathrm{I}_j(\boldsymbol{x}) \quad (3)$$

where n is the number of monomial filter kernels in the filter definition. For a rational operator this description yields

$$\boldsymbol{y} = \boldsymbol{x} + \frac{\sum_{j=1}^{n} a_j \mathrm{I}_j(\boldsymbol{x})}{\sum_{k=1}^{m} a_k \mathrm{I}_k(\boldsymbol{x})} \; . \quad (4)$$

The separate term $\boldsymbol{x}$ in eqs. (3) and (4) does not restrict the generality of the expression but facilitates the reasoning in the following sections of this paper. The description based on monomial filter kernels guarantees isotropy and reduces significantly the number of filter coefficients present in eq. (1). In contrast to the heuristically determined filter descriptions it has the advantage of facilitating the analysis of the filters and the comparison of different filters.

3.2. Preservation of the expectation value

A further desired filter property is that the expectation value of an image $\boldsymbol{x}$ should remain the same for the processed image $\boldsymbol{y} = F(\boldsymbol{x})$ with the operator F:

$$\mathrm{E}\{\boldsymbol{y}\} = \mathrm{E}\{\boldsymbol{x}\} \; . \quad (5)$$

In the heuristic filter design this condition is usually tried to meet by constraining the sum of the coefficients to be zero [5]:

$$\sum_{j=1}^{n} a_j = 0 \; . \quad (6)$$

However, this is only valid if the expectation values of all monomial filter kernels are identical. For nonlinear filter kernels this equation does not hold. As an example the expectation values of the monomial filter kernels of Table 1 applied to a constant image with value μ plus zero mean Gaussian noise with variance σ^2 are given in Table 2.

Order	Monomial	Mean
1	I1, I2	μ
2	I3, I4	$\mu^2 + \sigma^2$
	I5, I6, I7	μ^2
3	I8, I9	$\mu^3 + 3\sigma^2\mu$
	I10, I11, I12, I13, I14	$\mu^3 + \sigma^2\mu$
	I15, I16, I17	μ^3

Table 2: Expectation value of monomial filter kernels applied to constant images with mean μ distorted with added Gaussian noise $\mathcal{N}(0, \sigma)$

Therefore the correct constraint to fulfill eq. (5) in the general equation

$$\mathrm{E}\{\boldsymbol{y}\} \;=\; \mathrm{E}\{\boldsymbol{x}\} + \mathrm{E}\left\{\sum_{j=1}^{n} a_j \mathrm{I}_j(\boldsymbol{x})\right\}$$

for the expectation value of the filtered image is that the expectation value of the correction term added to the image must be equal to zero:

$$0 \;=\; \mathrm{E}\left\{\sum_{j=1}^{n} a_j \mathrm{I}_j(\boldsymbol{x})\right\} \; . \quad (7)$$

Thus, an optimal polynomial filter for a given application can be designed by adapting the coefficients of the various monomial filter kernels due to a suitable optimization criterion under the constraint of eq. (7).

3.3. Edge detection

Another requirement of polynomial and rational filters for image enhancement applications is a reliable recognition of edges. For this purpose a highpass characteristic of the filter expressed by certain relationships between the filter coefficients is needed. A prerequisite for the derivation of generally valid constraints is that the expectation values of the monomial filter kernels are determinable on a formal basis. However, for nonlinear operators no assumptions can

Order	Monomials		
1	I1: $f_1 = x_{0,0}$	I2: $f_2 = x_{0,1}$	
2	I3: $f_3 = x_{0,0}^2$	I4: $f_4 = x_{0,1}^2$	I5: $f_5 = x_{0,0}x_{0,1}$
	I6: $f_6 = x_{0,1}x_{0,-1}$	I7: $f_7 = x_{0,1}x_{1,0}$	
3	I8: $f_8 = x_{0,0}^3$	I9: $f_9 = x_{0,1}^3$	I10: $f_{10} = x_{0,0}^2 x_{0,1}$
	I11: $f_{11} = x_{0,0}x_{0,1}^2$	I12: $f_{12} = x_{0,1}^2 x_{0,-1}$	I13: $f_{13} = x_{0,1}^2 x_{1,0}$
	I14: $f_{14} = x_{0,1}^2 x_{-1,0}$	I15: $f_{15} = x_{0,1}x_{0,0}x_{0,-1}$	I16: $f_{16} = x_{0,1}x_{-1,0}x_{0,-1}$
	I17: $f_{17} = x_{0,1}x_{0,0}x_{1,0}$		

Table 1: Monomial filter kernels based on monomials of up to order three

be made for an arbitrary distorted image [3]. As a consequence constraints can only be derived for linear filter kernels. A possible constraint to assure the detection of edges consists in applying a weighting of the linear monomial filter kernels in such a way that their linear combination shows the characteristic of a Laplace operator. For the scheme of filter kernels of Table 1 this constraint yields

$$-4a_1 = a_2 \; . \qquad (8)$$

For rational operators this constraint has to be fulfilled for the monomial filter kernels in the numerator.

4. EXPERIMENTAL RESULTS

For edge preserving noise smoothing the aim is to minimize the perceived difference between the filtered noisy image $\boldsymbol{y}$ and the original undistorted image $\boldsymbol{s}$. It can be achieved by minimizing the mean square error between these two images. This optimization criterion by itself applied on filters according to eq. (3) or eq. (4) already leads to an approximation of the expectation value of the difference image towards zero:

$$\text{minimize}_{a_i} \frac{\sum(\boldsymbol{y}(a_i) - \boldsymbol{s})^2}{\#\text{pixel}} \Rightarrow \mathrm{E}\{|\boldsymbol{y}(a_i) - \boldsymbol{s}|\} \rightarrow 0 \; . \qquad (9)$$

To show that this optimization criterion is already sufficient to fulfill the condition of eq. (5) experiments are per-

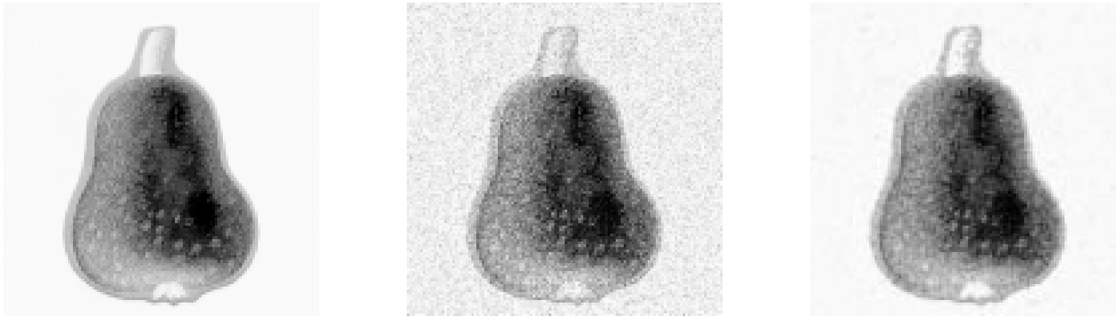

a) pear b) distorted, SNR 9 c) filtered with a rational operator

Figure 3: Image “pear” filtered with an optimized rational filter kernel

method	mean square error
polyn. filter based on 9 monomial filter kernels, unconstrained	233
polyn. filter based on 9 monomial filter kernels, eq. (7)	233
polyn. filter based on 9 monomial filter kernels, eq. (6)	234
polyn. filter based on 17 monomial filter kernels, unconstrained	227
polyn. filter based on 17 monomial filter kernels, eq. (7)	227
polyn. filter based on 17 monomial filter kernels, eq. (6)	233
rational filter, unconstrained	203
rational filter, eq. (7)	203
rational filter, eq. (6)	220

Table 3: Mean square error for the application of polynomial and rational filters on the image “pear”

formed on a real gray value image “pear” with added zero mean Gaussian noise (SNR=9). We apply different polynomial and rational filters three times to increase the smoothing ability. The obtained mean square error is given in Table 3 for the unconstrained optimization, the optimization under the constraints of eq. (6), and of eq. (7) for a polynomial filter based on 9 and 17 monomial filter kernels, and a rational operator with a cubic polynomial in the numerator and a quadratic polynomial in the denominator.

Figure 3 c) presents the result for the rational filter in comparison to the original image and the distorted one. The edge preservation and the smoothing ability are clearly visible.

All filter outputs yield the desired expectation value of $E\{|\boldsymbol{y}-\boldsymbol{s}|\} \approx 0$. No visible difference can be recognized between the results of the optimization with the mean square error criterion without constraints and the constraint of eq. (7). The obtained mean square errors are the same. Moreover these mean square errors are lower than those achieved with the unfounded constraint of eq. (6) for all tested edge preserving noise smoothing filters. The improvement is most evident for the rational operator.

Experiments with different images have also shown that in most cases the minimization of the mean square error between the filtered noisy image $\boldsymbol{y}$ and the original undistorted image $\boldsymbol{s}$ satisfies the constraint of eq. (8) for edge detection, too. Nearly equal values for the coefficients $-4a_1$ and a_2 are derived, respectively. However, it can be observed that for images containing just a small number of edges a minimum for the mean square error is found with values for the coefficients that do not satisfy eq. (8). As an example Table 4 shows the values for the coefficients a_1 and a_2 obtained from the optimization of the unconstrained versions of the three different above mentioned filters on the image “pear”.

For a comparison the derived mean square errors after a single application of these filters with the results of the same filters where the constraint of eq. (8) is explicitly applied are given. Although the values for the two coefficients for the unconstrained version of a polynomial filter based on 17 monomial filter kernels differ significantly from each other the improvement of the obtained mean square error with respect to the constrained version of the same filter is only neglectable.

Thus, the proposed unconstrained method of minimizing the mean square error applied for edge preserving noise smoothing in most cases yields a satisfaction of the design constraints derived for polynomial and rational filters. For images with few edges the constraint of eq. (8) may not be satisfied but without significantly improving the quality of

method	$4a_1$	a_2	mean square error
polyn. filter, 9 mon. filter kernels, unconst.	-0.089	0.089	278
polyn. filter, 9 mon. filter kernels, eq. (8)	-0.089	0.089	278
polyn. filter, 17 mon. filter kernels, unconst.	-0.161	0.101	269
polyn. filter, 17 mon. filter kernels, eq. (8)	-0.149	0.149	271
rational filter, numerator unconst.	-0.103	0.098	230
rational filter, numerator eq. (8)	-0.104	0.104	231

Table 4: Values of the coefficients a_1 and a_2, and mean square error for the application of polynomial and rational filters once on the image "pear"

the filtered image in terms of the mean square error. Summarizing the experiments have shown that the derived constraints are suitable for the design of polynomial and rational filters with certain defined properties.

5. CONCLUSION

General constraints for the design of polynomial and rational filters have been derived. These constraints guarantee isotropy, the preservation of the expectation value of the filtered image, and the detection of edges. These are desired characteristics of these filters for image processing applications.

For the application of edge preserving noise smoothing a method has been presented to find an optimal filter that meets the derived constraints for most images. It consists in the unconstrained optimization of the coefficients of a polynomial or rational filter with respect to the minimization of the mean square error between the noisy image and the original image.

6. ACKNOWLEDGEMENT

This work has been supported by a Marie Curie Fellowship from the European Commission within the program "Training and Mobility of Researchers", and by the University of Trieste.

7. REFERENCES

[1] Guillon, S. et al., *Adaptive nonlinear filters for 2D and 3D image enhancement*, Signal Processing, vol. 67, pp. 237-254, 1998

[2] Kröner, S.; Ramponi, G., *Edge Preserving Noise Smoothing with an Optimized Cubic Filter*, In: Tasic, J.F.; Burnik, U. (Eds.): Proc. of COST # 254 International Workshop on Intelligent Communications and Multimedia Terminals, pp. 3-6, Ljubljana, 19.-21. November 1998

[3] Lloyd, E., *Handbook of applicable mathematics*, Vol. II: Probability, Wiley, 1980

[4] Mo, S.; Mathews, J.V., *Adaptive, Quadratic Preprocessing of Document Images for Binarization*, IEEE Trans. on Image Processing, Vol. 7, No. 7, pp. 992-999, July 1998

[5] Ramponi, G. *Bi-impulse response design of isotropic quadratic filters*, Proc. IEEE, Vol. 78, No. 4, pp. 665-677, April 1990

[6] Ramponi, G., *The rational filter for image smoothing*, IEEE Signal Processing Letters, Vol. 3, No. 3, pp. 63 - 65, March 1996

[7] Ramponi, G., *A Cubic Unsharp Masking Technique for Contrast Enhancement*, Signal Processing, vol.67, no.2, pp.211-222, June 1998

[8] Ramponi, G., *Warped Distance for Space-Variant Linear Image Interpolation*, IEEE Trans. on Image Processing, Vol.8, No. 5, May 1999, to be published

[9] Ramponi G.; Carrato, S., *Interpolation of the DC Component of Coded Images Using a Rational Filter*, Proc. Fourth IEEE Intern. Conf. on Image Processing, ICIP-97, S. Barbara, CA, Oct. 26-29, 1997